



LAWRENCE
LIVERMORE
NATIONAL
LABORATORY

Direct correlation of R-line luminescence with rod-like defect evolution in ion-implanted and annealed silicon

S. Charnvanichborikarn, J. Wong-Leung, C.
Jagadish, J. S. Williams

July 22, 2011

MRS Communications

Disclaimer

This document was prepared as an account of work sponsored by an agency of the United States government. Neither the United States government nor Lawrence Livermore National Security, LLC, nor any of their employees makes any warranty, expressed or implied, or assumes any legal liability or responsibility for the accuracy, completeness, or usefulness of any information, apparatus, product, or process disclosed, or represents that its use would not infringe privately owned rights. Reference herein to any specific commercial product, process, or service by trade name, trademark, manufacturer, or otherwise does not necessarily constitute or imply its endorsement, recommendation, or favoring by the United States government or Lawrence Livermore National Security, LLC. The views and opinions of authors expressed herein do not necessarily state or reflect those of the United States government or Lawrence Livermore National Security, LLC, and shall not be used for advertising or product endorsement purposes.

Direct correlation of *R*-line luminescence with rod-like defect evolution in ion-implanted and annealed silicon

S. Charnvanichborikarn,^{1,2, a)} J. Wong-Leung,^{2,3} C. Jagadish,² and J. S. Williams²

¹⁾*Lawrence Livermore National Laboratory, Livermore, California 94550*

²⁾*Department of Electronic Materials Engineering, Research School of Physics and Engineering, The Australian National University, Canberra, ACT 0200, Australia*

³⁾*Centre for Advanced Microscopy, The Australian National University, Canberra, ACT 0200, Australia*

(Dated: 18 July 2011)

A quantitative correlation between *R*-line luminescence at around $1.37\ \mu\text{m}$ and $\{311\}$ defect nature, size, and concentration has been undertaken in silicon, following keV Si-implantation and subsequent annealing using photoluminescence spectroscopy and plan-view transmission electron microscopy. The formation and evolution of the rod-like defects were found to be dependent on annealing time at a temperature of $700\ ^\circ\text{C}$ but there was no simple correlation found between the density and size of those defects and the *R*-line intensity. In particular, whereas the presence of $\{311\}$ defects is essential for observing *R*-line luminescence, both very small $\{311\}$ defects at short annealing times and fully developed $\{311\}$ defects at long annealing times do not contribute to such luminescence. We provide possible explanations for this behavior and suggest that the local (strain) environment around defects, the dopant level and impurities in the silicon substrate may all play a role in determining *R*-line intensity.

PACS numbers: 78.55.Ap

^{a)}Electronic mail: charnvanichb1@llnl.gov

The process of ion implantation in silicon produces damage and defects that usually undergo extensive diffusion, annihilation and agglomeration during heat treatment.¹ Some of the residual defects following annealing are optically active when excited by photons or electrons.^{2,3} In such cases, the defects give rise to a defect state within the bandgap of silicon which allows a direct sub-bandgap transition and the emission of light. In particular, the interstitial-based defects (clusters and extended defects) in silicon can be optically active.² As the ion-implantation fluence and annealing temperature are raised, the residual defects evolve into interstitial defect clusters, rod-like defects (RLDs), and ultimately dislocations. The tri-Si-interstitial clusters, for example, are thought to be the origin of the *W*-line emission at 1218 nm.⁴⁻⁶ The $\{311\}$ RLDs are associated with *R*-line luminescence at 1372 nm,^{2,7} while dislocations are associated with so called D-bands at wavelengths above 1500 nm. The $\{311\}$ RLDs have received much interest in the past decade mainly due to their ability to facilitate transient enhanced diffusion (TED) of boron, a common *p*-type dopant in silicon, when they dissociate to release a flux of Si-interstitials.⁸ A comprehensive understanding of the TED process in the presence of $\{311\}$ RLDs has become increasingly important as devices shrink to a sub-micron scale. Apart from this obvious technological importance, the structural and optical properties of $\{311\}$ RLDs have also been of interest,^{1,2} the latter for the possibility of enhancing light emission from silicon.⁹ Previous studies have shown that the $\{311\}$ defect is a chain of Si-interstitials with a $\{311\}$ habit plane and extending along the $\langle 110 \rangle$ direction.¹⁰ Their formation takes place after Si-implantation at sub-amorphizing fluences of the order of 10^{13} cm^{-2} and following annealing at a temperature between 600 and 850 °C.¹¹⁻¹³ In addition, Chou *et al.* further reported that a small proportion of the RLDs (14%) had a $\{111\}$ habit plane.¹⁴ Although, $\{311\}$ RLDs have been proposed to be responsible for the *R*-line emission,^{11,15} no quantitative correlation has yet been made between the *R*-line intensity and the nature (size and density) of RLDs and their environment. The current study addresses this issue.

In this work, photoluminescence (PL) and transmission electron microscopy (TEM) are used to monitor both the evolution and intensity of the *R*-line luminescence and to quantify the average concentration and nature (size) of implantation-induced RLDs as a function of annealing time. We find that there is no simple correlation between the *R*-line intensity and the RLD size or density, despite the fact that the presence of RLDs is essential for *R*-line luminescence. We suggest that the *R*-line intensity also appears to be sensitive to other effects such as local strain, the nature of disorder surrounding $\{311\}$ defects or impurity effects.

Cz-grown boron-doped p-type (100) Si wafers with a resistivity of 5-25 $\Omega\text{-cm}$ were irradiated at room temperature with 80 keV Si^- ions to a fluence of $5 \times 10^{13} \text{ cm}^{-2}$, which produces a large number of excess Si-interstitials and subsequent $\{311\}$ defects beyond the ion projected range after annealing. We note that the chosen fluence is below a silicon amorphization threshold and was found to provide the optimum conditions for maximum *R*-line intensity for the ion energy used. The average scanned ion flux was kept constant at $3.45 \times 10^{11} \text{ cm}^{-2} \text{ s}^{-1}$ to prevent unnecessary substrate heating. The implanted wafer was cut into several 3 mm diameter discs using a Gatan 601 ultrasonic cutter. A post-implantation anneal was then carried out for each sample in N_2 ambient with a fixed flow rate of $\approx 0.65 \text{ lt/min}$ from 10 to 90 minutes at 700 $^\circ\text{C}$, where the sample was both inserted into and removed rapidly from the pre-heated furnace zone to promote rapid thermal ramping and cooling rates. Following annealing, the samples were mounted on a cryostat holder suitable for PL measurements and cooled to 13 K, where a 10 mW 532 nm laser was used to excite the luminescence. The PL spectra were dispersed by a SpectraPro-2500i triple grating monochromator equipped with a temperature-controlled InGaAs infrared photodetector. These same samples were used to prepare plan-view TEM specimens. The disc-shaped samples were mechanically thinned and dimpled from the backside down to about 10 μm at the center. Chemical etching was performed to perforate the samples, yielding large electron transparent regions. A Philips CM300 electron microscope operated at 300 kV was used to characterize all the TEM specimens. All the TEM images were recorded under a weak-beam dark field (WBDF) condition using a $g\text{-}ng$ diffraction arrangement, where $g = 022$ and $n = 3.2$. This imaging condition was used to survey the defect density but detailed Burgers vector determination of the RLDs were not carried out within the scope of this work. The inclination of the defect lines with respect to the TEM foil (as observed by a dotted contrast)¹⁶ is also taken into account when determining the size of the defect.

Figure 1 shows the PL spectra measured at 13 K from the Si-implanted samples isothermally annealed at 700 $^\circ\text{C}$ for different time periods from 10 to 90 minutes. The signal from silicon band-edge luminescence Si_{TO} at 1130 nm is observed in all the spectra and becomes brighter with increasing annealing time, as a result of a progressive reduction in the overall implantation-induced disorder. Annealing for 10 minutes results in a small but broad peak centered around 1350 nm, and a larger and broader feature beyond 1400 nm. Unlike the Si_{TO} , the *R*-line luminescence is only observed after annealing from 20 to 60 minutes. Indeed, the *R*-line is maximized in intensity by 40 minutes and disappears completely by 90 minutes. At first sight, the loss of *R*-line intensity

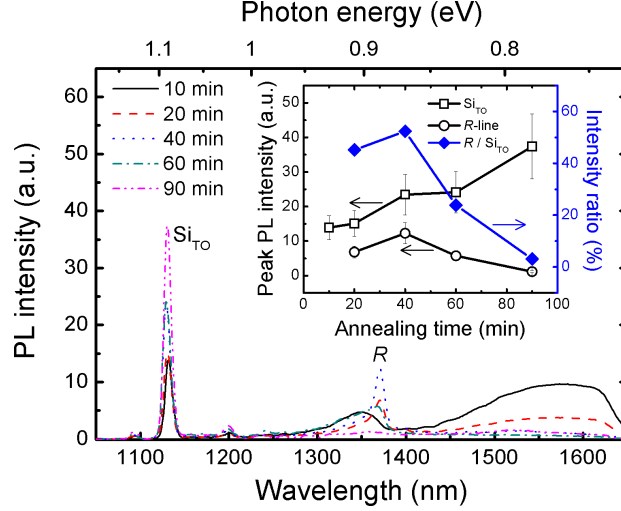


FIG. 1. (Color online) PL spectra for silicon samples implanted with 80 keV Si ions to a fluence of $5 \times 10^{13} \text{ cm}^{-2}$ and a subsequent anneal at 700 °C for various times. The inset displays intensities of a silicon peak (open squares) and the *R*-line (open circles) as a function of annealing time. The intensity ratio of the *R*-line to silicon peak (solid diamonds) is plotted in the right ordinate.

after 90-minute annealing is in disagreement with a previous study, where a strong *R*-line was observed after annealing at 700 °C for at least an hour.¹⁷ However, the implantation regime used in this previous study (1.2 MeV Si to a fluence of 10^{13} cm^{-2}) is expected to initiate a different defect evolution pathway during annealing from that in our study.

We note after 60-minute annealing that the *R*-line peak is not only lower in intensity but also slightly shifted to shorter wavelength. It is also noteworthy that a longer wavelength broad luminescence band (from 1425 to 1650 nm) is observed in most of the cases, and is particularly strong at annealing times ≤ 20 minutes. Thus, it is tempting to speculate that this broad feature may arise from either small interstitial clusters¹⁸ or strained regions¹⁹ that have not fully evolved into extended defects, a fact that is clarified later by TEM.

In order to interpret the PL spectra, it is important to treat the effect of implantation damage carefully. The process of ion-implantation usually introduces lattice damage that contributes to the formation of non-radiative recombination centers, leading to an overall loss of luminescence intensity. Harding *et al.* have suggested that the effect of radiation damage may be gauged by examining the intensity of the relevant peak (*R*-line) relative to the silicon (Si_{TO}) peak.²⁰ The inset of Fig. 1 plots the PL peak intensities of the *R*-line (open circles) and Si_{TO} (open squares) peak against the annealing time, while the intensity ratio of the *R*-line to Si_{TO} for each annealing time

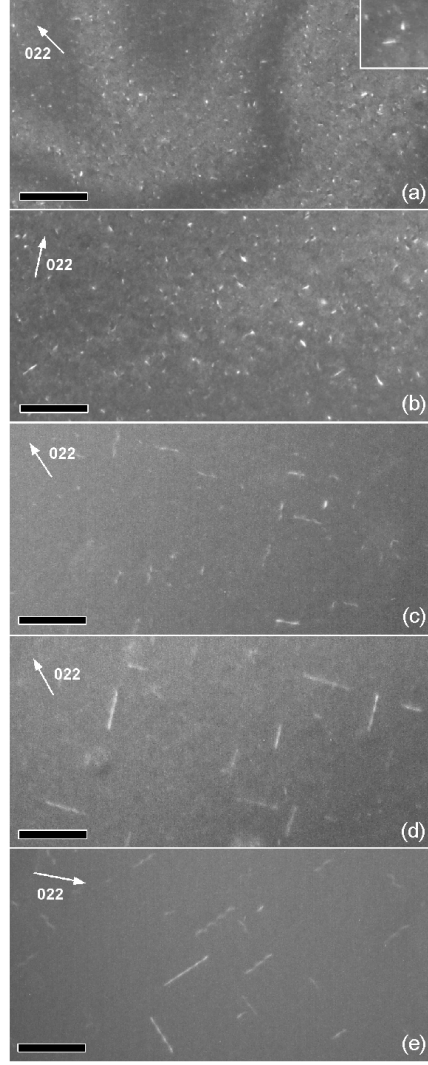


FIG. 2. WBDF micrographs illustrating in plan view RLDs formed in silicon by 80 keV Si-ion implantation and subsequent 700 °C annealing for (a) 10 minutes, (b) 20 minutes, (c) 40 minutes, (d) 60 minutes, and (e) 90 minutes. The scale bars represent 100 nm.

is shown with respect to the right-hand axis. Clearly, the R -line intensity drops after 40 minutes, whereas the Si_{TIO} increases as the implantation damage is removed.

Figure 2 shows representative plan-view TEM images of the corresponding samples. The RLDs exist in all samples, however, they are not well formed and are very dilute in the 10-minute annealed sample (Fig. 2(a)). Indeed, most of the defects observed after 10-minute annealing are nanometer-sized clusters, which may be regarded as possible precursors of the RLDs. The inset of Fig. 2(a) shows a close-up image of embryonic RLDs and clearly indicates a preferential line orientation in spite of its short dimension. The other samples annealed from 20 to 90 minutes

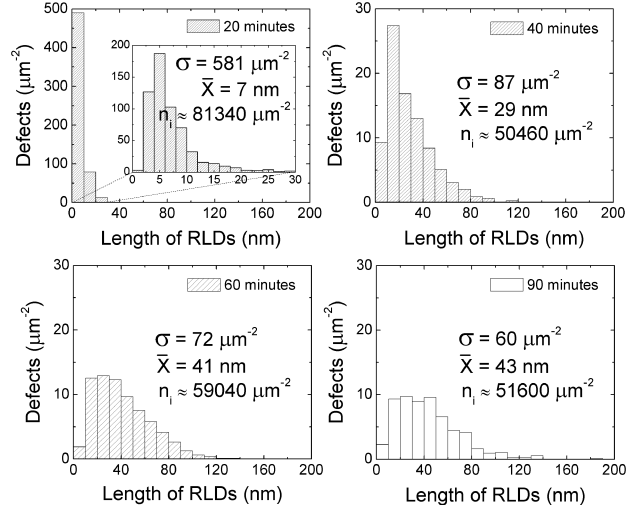


FIG. 3. Statistical collection illustrating the size and density of the RLDs distributed after annealing at 700 °C for 20 to 90 minutes.

are illustrated in Figs. 2(b)–(e). In fact, the RLDs can clearly be found to elongate in $\langle 110 \rangle$ directions after annealing for 40 minutes. The size distribution of the RLDs are compared for the various annealing times in Fig. 3.

As shown in Fig. 3, the defect distribution changes significantly with increasing annealing time. These interstitial-based RLDs gradually grow (at a non-linear rate) with time up to 60 minutes but their average length (\bar{X}) remains virtually constant on further annealing, consistent with a previous finding.²¹ The RLD concentration (σ), on the other hand, decreases abruptly during the 20- to 40-minute period but more slowly upon prolonged annealing. This observation suggests a growth of the RLDs, and the liberation of interstitials during the anneal.^{22,23} Assuming that 1 nm of a RLD contains 20 interstitials^{22,24}, it is possible to estimate the number of Si-interstitials (n_i) involved in RLDs from the distributions, which is given in each case in Fig. 3. The loss of interstitials from the RLDs during growth and dissolution is about 30% between 20 and 40 minutes and becomes less significant for further annealing up to 90 minutes.

Previous work has correlated the *R*-line luminescence to the presence of the $\{311\}$ defects.¹¹ However, the present study has provided a quantitative correlation that illustrates that the presence of $\{311\}$ defects alone is not sufficient to guarantee *R*-line luminescence. In our case, where the majority of defects appear to be ill-defined interstitial clusters in the 10-minute annealed samples, the lack of *R*-line luminescence may be a result of the small size of the $\{311\}$ defects. Indeed, Schmidt *et al.* have argued that *R*-line luminescence is not observed in samples containing very

TABLE I. Defect density and *R*-line luminescence intensity for different annealing times.

Annealing time (min)	Defect density (μm^{-2})		<i>R</i> / Si _{TO} (%)
	≤ 5 nm	> 5 nm	
10	-	-	-
20	372	523	95.2
40	4	678	122.2
60	0	573	49.5
90	0	448	2.8

short $\{311\}$ defects of size $\lesssim 5$ nm.⁷ Thus, a more complex explanation is required to explain the disappearance of the *R*-line (and the evolution of the luminescence spectrum) for the 90-minute anneal since there is little change in the size and density of the RLDs between the 60- and 90-minute annealed cases. Furthermore, the intensities of the *R*-line luminescence in the 20- and 40-minute annealed samples are comparable (within a factor of 2) although the distribution profiles of the RLDs are widely different. Specifically, the sample annealed for 20 minutes contains a high concentration of short RLDs, while those in the sample annealed for 40 minutes are undoubtedly fewer and much longer (see Fig. 3). This suggests that RLDs of different sizes may contribute unequally to the *R*-line luminescence.

Based on the above results, an explanation of *R*-line luminescence based solely on an optimum RLD size is questionable. Furthermore, the estimated total number of Si-interstitials that are trapped in RLDs in 60- and 90-minute anneal cases is similar, hence the *R*-line intensity does not scale with the number of Si interstitials. Let us now explore some other possibilities to explain our results such as strain-stimulated luminescence from $\{311\}$ defects and the role of competing quenching mechanisms that can decrease the *R*-line intensity.

Firstly, local strain surrounding defects has previously been proposed as a contributing factor in radiative recombination associated with RLDs that gives rise to the *R*-line.¹⁵ Although our TEM analysis of strain fields around the defects could not be quantified, it remains possible that strain surrounding $\{311\}$ defects, and its relaxation at longer annealing times can explain our results. Secondly, as shown in Table I, the concentration of $\{311\}$ defect sizes < 5 nm is highest after 20-minute annealing and decreases abruptly with increasing annealing time. The concentration of larger $\{311\}$ defects (> 5 nm), on the other hand, increases with annealing time up to 40 minutes

and then decreases, which follows the trend of the R/S_{TO} intensity ratio but the latter decreases well over an order of magnitude more rapidly. This observed relationship is in agreement with the previous finding that the small size $\{311\}$ defects (≤ 5 nm), of which surrounding strain may not have fully developed, do not give rise to the R -line.⁷ However, the intensity ratio of the R -line decreases at a much faster rate than the evaporation of the large RLDs (> 5 nm). It is possible that the prolonged anneal may lead to a state where the surrounding strain is reduced as the RLDs further develop and is not sufficient to assist exciton recombination at the defect sites. Finally, processes competing with luminescence from $\{311\}$ defects such as other non-radiative recombination centers associated with irradiation damage²⁰, quenching by dopant effects and trapping of impurities at defects^{25,26} may play an important role, especially at long annealing times. For example, gettering of (metal) impurities to dislocations has previously been suggested as a possible cause for observed changes in band-edge luminescence.^{27,28}

In summary, we have conducted experiments to quantitatively investigate the link between R -line luminescence and physical properties of the corresponding RLDs formed by Si-implantation and thermal annealing. Our observations suggest that the relationship between the RLD size and density and R -line luminescence intensity is complicated, whereby very small RLDs under 5 nm contribute minimally to the R -line intensity. Other factors such as the local strain surrounding the defect regions and residual damage, dopant effects or impurities could potentially influence detection of the R -line at longer annealing times.

One of the authors (S.C.) thanks Bianca Haberl for assistance in TEM sample preparation. This work was funded by the Australian Research Council. This work was performed under the auspices of the U.S. DOE by LLNL under Contract DE-AC52-07NA27344.

REFERENCES

- ¹S. Libertino and A. La Magna, in *Materials Science with Ion Beams*, Topics in Applied Physics Vol. 116, edited by H. Bernas (Springer-Verlag, Berlin 2010), p. 147.
- ²G. Davies, Phys. Rep. **176**, 83 (1989).
- ³S. Charnvanichborikarn, Ph.D. thesis, The Australian National University, 2011.
- ⁴G. Davies, E. C. Lightowers, and Z. E. Ciechanowska, J. Phys. C **20**, 191 (1987).
- ⁵B. J. Coomer, J. P. Goss, R. Jones, S. Öberg, and P. R. Briddon, Physica B **273–274**, 505 (1999).
- ⁶P. K. Giri, Semicond. Sci. Technol. **20**, 638 (2005).

- ⁷D. C. Schmidt, B. G. Svensson, M. Seibt, C. Jagadish, G. Davies, J. Appl. Phys. **88**, 2309 (2000).
- ⁸D. J. Eaglesham, P. A. Stolk, H.-J. Gossmann, and J. M. Poate, Appl. Phys. Lett. **65**, 2305 (1994).
- ⁹Y. Yasutake, J. Igarashi, N. Tana-ami, and S. Fukatsu, Opt. Express **17**, 16739 (2009).
- ¹⁰M. D. Matthews and S. J. Ashby, Philos. Mag. **27**, 1313 (1973).
- ¹¹S. Coffa, S. Libertino, and C. Spinella, Appl. Phys. Lett. **76**, 321 (2000).
- ¹²P. K. Giri, S. Coffa, and E. Rimini, Appl. Phys. Lett. **78**, 291 (2001).
- ¹³G. Davies, R. Harding, T. Jin, A. Mainwood, and J. Leung-Wong, Nucl. Instrum. Methods Phys. Res. B **186** 1 (2001).
- ¹⁴C. T. Chou, D. J. H. Cockayne, J. Zou, P. Kringhøj, C. Jagadish, Phys. Rev. B **52**, 17223 (1995).
- ¹⁵E. C. Lightowers, L. Jeyanathan, A. N. Safonov, V. Higgs, and G. Davies, Mater. Sci. Eng., B **24**, 144 (1994).
- ¹⁶J. Wong-Leung, S. Fatima, C. Jagadish, J. D. Fitz Gerald, C. T. Chou, J. Zou, and D. J. H. Cockayne, J. Appl. Phys. **88**, 1312 (2000).
- ¹⁷S. Libertino, S. Coffa, C. Spinella, A. La Magna, V. Privitera, Nucl. Instrum. Methods Phys. Res. B **178**, 25 (2001).
- ¹⁸N. E. B. Covern, G. Mannino, P. A. Stolk, F. Roozeboom, H. G. A. Huizing, J. G. M. van Berkum, F. Cristiano, A. Claverie, and M. Jaraíz, Phys. Rev. Lett. **82**, 4460 (1999).
- ¹⁹H. Weman, B. Monemar, G. S. Oehrlein, and S. J. Jeng, Phys. Rev. B **42**, 3109 (1990).
- ²⁰R. E. Harding, G. Davies, S. Hayama, P. G. Coleman, C. P. Burrows, and J. Wong-Leung, Appl. Phys. Lett **89**, 181917 (2006).
- ²¹K. Moller, K. S. Jones, and M. E. Law, Appl. Phys. Lett. **72**, 2547 (1998).
- ²²P. A. Stolk, H.-J. Gossmann, D. J. Eaglesham, D. C. Jacobson, C. S. Rafferty, G. H. Gilmer, M. Jaraíz, J. M. Poate, H. S. Luftman, and T. E. Haynes, J. Appl. Phys. **81**, 6031 (1997).
- ²³G. Z. Pan and K. N. Tu, J. Appl. Phys. **82**, 601 (1997).
- ²⁴S. Takeda, Jpn. J. Appl. Phys. **30**, L639 (1991).
- ²⁵T. E. Haynes, D. J. Eaglesham, P. A. Stolk, H.-J. Gossmann, D. C. Jacobson, and J. M. Poate, Appl. Phys. Lett. **69**, 1376 (1996).
- ²⁶R. Brindos, P. Keys, K. S. Jones, and M. E. Law, Appl. Phys. Lett. **75**, 229 (1999).
- ²⁷V. Higgs, E. C. Lightowers, C. E. Norman, and P. Kightley, Mater. Sci. Forum **83–87**, 1309 (1992).
- ²⁸A. N. Tereshchenko, E. A. Steinman, and A. A. Mazilkin, Phys. Solid State **53**, 369 (2011).